Nanodiamonds with photostable, sub-gigahertz linewidth quantum emitters

Toan Trong Tran, Mehran Kianinia, Kerem Bray, Sejeong Kim, Zai-Quan Xu, Angus Gentle, Bernd Sontheimer, Carlo Bradac, and Igor Aharonovich

Citation: APL Photonics **2**, 116103 (2017); doi: 10.1063/1.4998199

View online: https://doi.org/10.1063/1.4998199

View Table of Contents: http://aip.scitation.org/toc/app/2/11

Published by the American Institute of Physics

Nanodiamonds with photostable, sub-gigahertz linewidth quantum emitters

Toan Trong Tran,[1,a] Mehran Kianinia,[1] Kerem Bray,[1] Sejeong Kim,[1] Zai-Quan Xu,[1] Angus Gentle,[1] Bernd Sontheimer,[2] Carlo Bradac,[1] and Igor Aharonovich[1]

[1]*School of Mathematical and Physical Sciences, University of Technology Sydney, Ultimo, NSW 2007, Australia*

[2]*Institute for Physics, Humboldt-University of Berlin, Berlin, Germany*

(Received 28 July 2017; accepted 16 October 2017; published online 7 November 2017)

Single-photon emitters with narrow linewidths are highly sought after for applications in quantum information processing and quantum communications. In this letter, we report on a bright, highly polarized near infrared single photon emitter embedded in diamond nanocrystals with a narrow, sub-GHz optical linewidth at 10 K. The observed zero-phonon line at ~780 nm is optically stable under low power excitation and blue shifts as the excitation power increases. Our results highlight the prospect for using new near infrared color centers in nanodiamonds for quantum applications. https://doi.org/10.1063/1.4998199

I. INTRODUCTION

Solid-state single-photon emitters (SPEs) such as quantum dots or defects in solids are becoming prominent candidates for realization of scalable quantum information technologies.[1–4] In particular, color centers in diamonds are one of the most attractive candidates for quantum applications due to their optical stability and availability of spin photon interfaces.[5–7]

Whilst there are hundreds of luminescent defects known to be hosted in diamonds, the vast majority of the existing studies focus on the negatively charged nitrogen-vacancy (NV) center. Yet, the NV center has a major drawback, as only ~4% of the photons are emitted into the zero-phonon line (ZPL).[8] This hinders its potential use in scalable nanophotonics devices and demands for sophisticated cavity engineering solutions.[9–11] As a result, other types of diamond color centers with narrow lines and high Debye-Waller factors have been recently investigated. These include the silicon vacancy (SiV) center,[12–17] the germanium vacancy (GeV) center,[18–20] and other emitters at the near infrared (NIR) spectral range.[21–23]

In this work, we explore the optical properties and the linewidth of SPEs embedded in nanodiamonds grown via chemical vapor deposition (CVD). At room temperature, the emitters have linewidths of ~2 THz (~4 nm) and a range of ZPLs at the NIR with extremely high Debye-Waller factors. When cooled down to 10 K, most of the emitters show spectrometer-limited lines. These properties make the emitters extremely promising for a variety of quantum photonic applications. In particular, we show that the emitters exhibit sub-GHz linewidths within nanodiamonds (NDs), which offers interesting possibilities for the potential realization of hybrid quantum photonic networks.[24,25]

II. METHODS

The diamond nanocrystals were grown from detonation nanodiamond seeds (diameter 4-6 nm) that were spin coated on a sapphire substrate. The use of sapphire substrates assists in minimizing the

[a]E-mail: trongtoan.tran@student.uts.edu.au

incorporation of silicon atoms that would otherwise result in undesired silicon doping. The samples were then loaded into a microwave plasma chemical vapor deposition (MPCVD) system, and the crystals were grown in mixed gases (hydrogen:methane = 100:1) with a microwave power of 900 W, at 60 Torr of atmospheric pressure for 30 min. Under these conditions, nanodiamonds with diameters of ~0.3–1 μm were grown [Fig. 1(a)].

A continuous wave (CW) tunable Ti:sapphire laser (M Squared Ltd.) was used for excitation and scanning. The laser was directed through a Glan-Taylor polarizer (Thorlabs, Inc.) and an achromatic half-waveplate (Thorlabs, Inc.), and focused onto the sample using a high numerical aperture (NA = 0.95, Nikon) objective lens. The sample stage was enclosed in a high vacuum chamber, equipped with an open-loop liquid helium flow system (ST500, Janis Ltd.). Scanning was performed using an X-Y piezo scanning mirror (FSM-300™). The sample was moved into place via a XYZ cryogenic-grade piezo stage (Attocube, Inc.). The collected light passed through a 90:10 (T:R) beamsplitter (Thorlabs, Inc.) and an additional long-pass filter (Semrock) to reject the residual

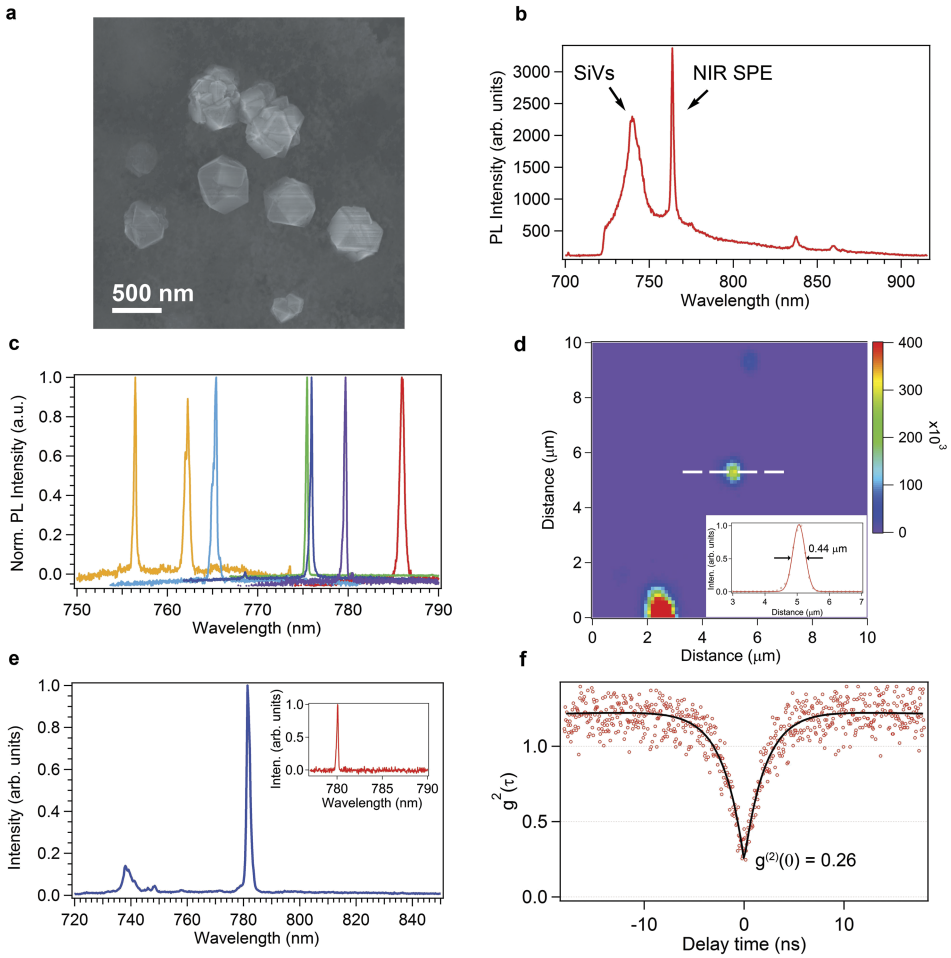

FIG. 1. (a) SEM image showing several MPCVD-grown nanodiamonds on a sapphire substrate. The nanodiamonds are ~0.3–1 μm in size. (b) A typical PL spectrum showing both SiVs and a near-infrared emitter recorded at room temperature. (c) ZPL distribution of the color centers in MPCVD-grown nanodiamonds analyzed in this study. A 700-nm, CW laser at 300 μW was used to excite the color centers at 80 K. (d) Confocal PL map recorded with 700-nm laser excitation at 300 μW with a bandpass filter (785 ± 22) nm and acquired at 10 K. The bright spot corresponds to a nanodiamond hosting a single emitter. The bottom inset shows the cross-sectional intensity analysis (dotted line) revealing a FWHM of 0.44 μm, consistent with emission from a point-source. (e) Normalized PL spectrum taken from the color center in (d) (blue trace) with a 300 g/mm grating. The inset (red trace) shows a higher resolution spectrum taken from the same emitter (with a 1800 g/mm grating). The measurements were conducted at 10 K. (f) Second-order autocorrelation function (red open circles) acquired for the emitter with a bandpass filter (785 ± 22) nm. The black solid line is the fitting (see main text) for the $g^{(2)}(0)$ function. The measurement was carried out at 80 K. The value of 0.26, without any background correction, indicates that the emission is from a single emitter.

pump. The signal was then coupled into a graded-index fiber, where the fiber aperture served as a confocal pinhole. A fiber splitter was used to direct the light to a spectrometer (Andor SR303i), equipped with both a 300 g/mm grating and a 1800 g/mm grating, or to two avalanche photodiodes (Excelitas Technologies™) arranged in a Hanbury-Brown and Twiss interferometer configuration. Correlation measurements were carried out using a time-correlated single-photon counting module (Swabian Time Tagger 20™). The presented $g^{(2)}(\tau = 0)$ curve displayed in Fig. 1(f) is not background-corrected.

Lifetime measurements were performed using a 675-nm pulsed laser excitation source (PiL067X™, Advanced Laser Diode Systems GmbH) with a 100-ps pulse width and 10-MHz repetition rate. The optical properties of the emitters were studied using a home-built laser scanning confocal photoluminescence (PL) microscope equipped with a continuous wavelength tunable titanium sapphire laser (linewidths, 100 kHz). The sapphire substrate with the grown diamond nanocrystals was mounted onto a cryostat equipped with a high-precision XYZ piezo scanning stage and was cooled to 10 K using liquid helium. The excitation and collection were done via a high numerical aperture (NA = 0.9) objective mounted inside the cryostat, creating an excitation and collection spot size of ~430 nm. The signal collected from the emitters was analyzed with both a spectrometer equipped with a high-resolution silicon-based charge coupled device (CCD) camera and a Hanbury-Brown and Twiss (HBT) interferometer.

III. RESULTS AND DISCUSSION

From surveying the confocal PL scans with a 700-nm laser excitation, we observed both ensembles of SiV centers and NIR single emitters [Fig. 1(b)]. The SiV centers embedded in the nanodiamonds exhibit emission at ~738 nm, whereas the NIR emitter, spectrally separated form SiV centers, emits at various longer wavelengths with sharp ZPLs. All the studied nanodiamonds exhibited SiV emitters but not all the nanodiamonds contained the bright isolated NIR emitters. A detailed spectroscopic study of the sample revealed that the nanodiamonds host narrowband color centers with a ZPL in the range of 756–786 nm [Fig. 1(c)]. Note that these are not the SiV defects but other NIR emitters. On average, two to three emitters were found in a $60 \times 60\ \mu m^2$ scan area, with the nanodiamond areal density of ~0.0125 particles/μm^2 (~45 particles per $60 \times 60\ \mu m^2$). Bright spots that correlate with single emitters embedded in the nanodiamonds are shown in Fig. 1(d). The cross-sectional analysis of each spot shows a Gaussian profile with a full-width-at-half-maximum (FWHM) of 0.44 μm, very close to the diffraction-limited point spread function of our confocal system (bottom right inset). For the remaining of the manuscript, we focus on a particular line at 780 nm. The line was selected arbitrarily, with the goal to study centers that emit further in the NIR. Consequently, Fig. 1(e) shows the narrow ZPL at 780 nm with a FWHM of ~79 GHz (~0.16 nm) that corresponds to our spectrometer resolution. The inset in Fig. 1(e) corresponds to the higher resolution spectrum of the same emitter. The spectra were recorded at 10 K. From the spectrum, we deduced a Debye-Waller (DW) factor, $DW = I_{ZPL}/I_{tot} = 0.87$, a value higher than that of the nitrogen-vacancy color center in diamonds (0.04) and comparable with that of SiV and GeV defects.

To verify that the center is indeed a single-photon emitter, a second-order autocorrelation function, $g^2(\tau)$, was recorded and is shown in Fig. 1(f). The data are fitted by employing a standard three-level model for the color center $g^{(2)}(\tau) = 1 - (1 + a)\, e^{-\tau/\tau_1} + a e^{-\tau/\tau_2}$, where a is the bunching factor, while τ_1 and τ_2 are the lifetimes of the excited and metastable states, respectively. The fit yields a value of 0.26 for $g^{(2)}(0)$, indicating the quantum nature of the emission. The non-zero antibunching dip is due to the timing jitter of our detectors, similarly to previous studies.[26–28] Under increasing excitation power, a slight photo-bunching was observed, indicating the presence of a third shelving state.

Additionally, we investigate the brightness and polarization of the chosen emitter. The saturation curve for the emitter with the ZPL at ~780 nm is shown in Fig. 2(a). A fitting based on the following equation is used to extract characteristic information about the emitter:

$$I = I_{\max} \times P/(P + P_{sat}),$$

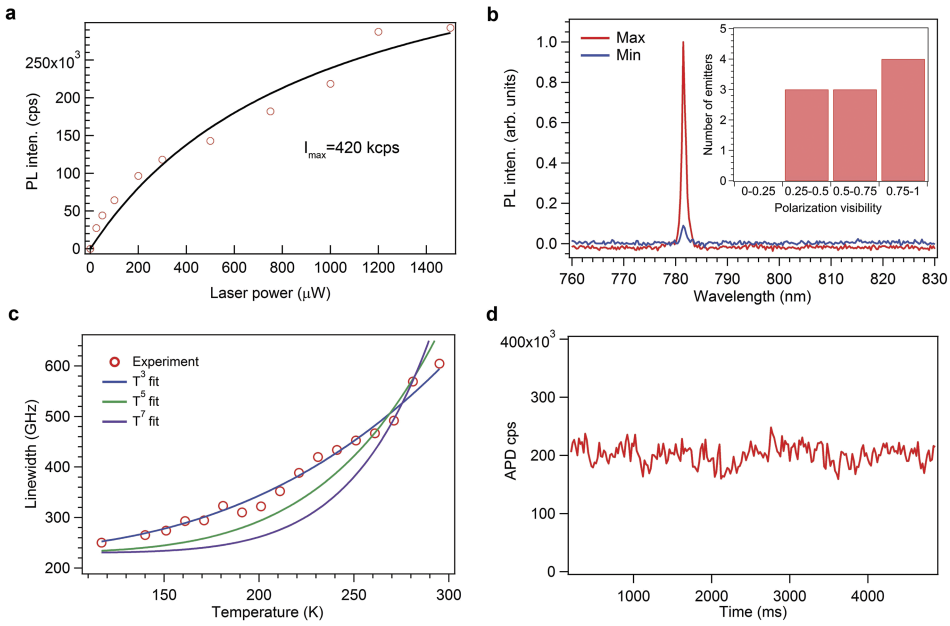

FIG. 2. (a) Power-dependent fluorescence saturation curve (red open circles). The fit (solid red line) produces values of $I_{\max}$, I_{sat}, and P_{sat} of 420 kcounts/s, 210 kcounts/s, and 960 μW, respectively. The measurement was acquired with a bandpass filter (785 ± 22) nm. (b) Spectra showing maximum (red trace) and minimum (blue trace) emission polarization from the emitter and taken with the use of a linear polarizer. The data were taken using excitation laser power of 300 μW with 5-s acquisition time. The visibility was determined to be 0.83. The inset shows a visibility statistic from 10 randomly chosen emitters. (c) Emission linewidth as a function of temperature for the emitter from 117 K to 295 K. The linewidths were obtained by fitting the Lorentzian function to the PL spectra. The experimental data are in red open circles while the blue, green, and purple solid lines are T^3, T^5, and T^7 power law fits, respectively. (d) Emission photostability as a function of time shows stable fluorescence. The bin time is 20 ms. The excitation wavelength and power are 700 nm and 1 mW, respectively. Measurements in (a), (b), and (d) were conducted at 10 K.

where $I_{\max}$ and P_{sat} are the maximum emission rate and excitation power at which saturation is reached, respectively. The fit produces values for $I_{\max}$, I_{sat}, and P_{sat} of 420 kcounts/s, 210 kcounts/s, and 960 μW, respectively. This level of brightness is superior to that of NV[29] and SiV[30] centers grown on a non-iridium substrate.

By rotating a linear polarizer at the collection path and measuring the intensity from the ZPL of the emitter, we obtain a visibility of 0.83 with the following expression [Fig. 2(b)]:

$$VIS = \frac{I_{\max} - I_{\min}}{I_{\max} + I_{\min}},$$

where $I_{\max}$ and $I_{\min}$ are the maximum integrated emission intensity and minimum integrated emission intensity, respectively. A visibility of almost unity indicates that the emission is associated with a single transitional dipole moment. The small deviation (0.17) from unity is attributed to an off-plane angular misalignment of the transition dipole moment with respect to the substrate. Furthermore, a visibility survey taken from 10 randomly chosen emitters [inset Fig. 2(b)] shows a distribution of values ranging from 0.29 to 0.92, with the average visibility value of 0.69. These statistical data, therefore, suggest that the orientation of the emitter's dipole moments is random—a typical observation from color center embedded nanodiamonds.[14]

Next, we measured the linewidth as a function of temperature (117–295 K) for the emitter to understand its phonon-coupling characteristic. Figure 2(c) presents the Lorentzian-fit linewidth values (red open circles) obtained at different temperatures as well as the T^3 (blue line), T^5 (green line), and T^7 (purple line) fits. The T^3 dependence describes the experimental data best, suggesting that the linewidth broadening from the emitter is mostly due to the coupling to low-energy phonons.[31]

Finally, we carried out a temporal PL intensity measurement at 1 mW excitation power to obtain the fluorescence intermittency characteristic of the emitter as shown in Fig. 2(d). The emitter remains stable even at higher excitation powers.

To gain more information about the coherent properties of the SPEs and unveil its natural linewidth, resonant excitation measurements were performed. While cross-polarization schemes are often used for studying quantum dots,[32] they were not practical in our measurement due to the high scattering from the diamond nanocrystals. To filter the excitation laser, we used a long-pass filter to collect only the emitter's phonon side band (PSB). Figure 3(a) shows a resonant excitation spectrum recorded at 5 μW with 5-GHz scan range and 70-MHz resolution of the same SPE as shown in Fig. 1 (center wavelength at 779.61 nm or 384.54 THz). A single peak was clearly observed. The data are fit with a Lorentzian profile, producing a FWHM of 660 MHz and as a comparison with a Gaussian line shape, that results in a linewidth of 800 MHz. Using χ^2 as the good-of-fit parameter, we obtained values of 6.53×10^6 and 6.71×10^6 for Lorentzian and Gaussian fits, respectively. From the fitting results, the Lorentzian fit arrived at slightly lower χ^2 values than that from the Gaussian fit. The Lorentzian line shape results in a better fit when compared to the Gaussian fit, suggesting that the optical linewidth is less prone to spectral diffusion.[22,33,34] However, given the rather close χ^2 values, at this stage, it is hard to conclude whether pure dephasing (i.e., due to phonon interactions) or spectral diffusions are the main contributors to the line broadening.

The excited state lifetime of the emitter was measured using a pulsed laser to find out whether the emitter's linewidth is Fourier-Transform (FT) limited. The results are shown in Fig. 3(b). Using a single-exponential fit, the lifetime of the excited state of the emitter was determined to be τ_1 = 1.1 ns. By applying the expression[35] $\gamma = 1/2\pi\tau_1$, where γ and τ_1 are the FT-limited linewidth (natural linewidth) and the excited state's lifetime of the emitter, respectively, we estimated a value for γ of 145 MHz. This means that the emitter's linewidth is ~4.5 times broader than the expected value.

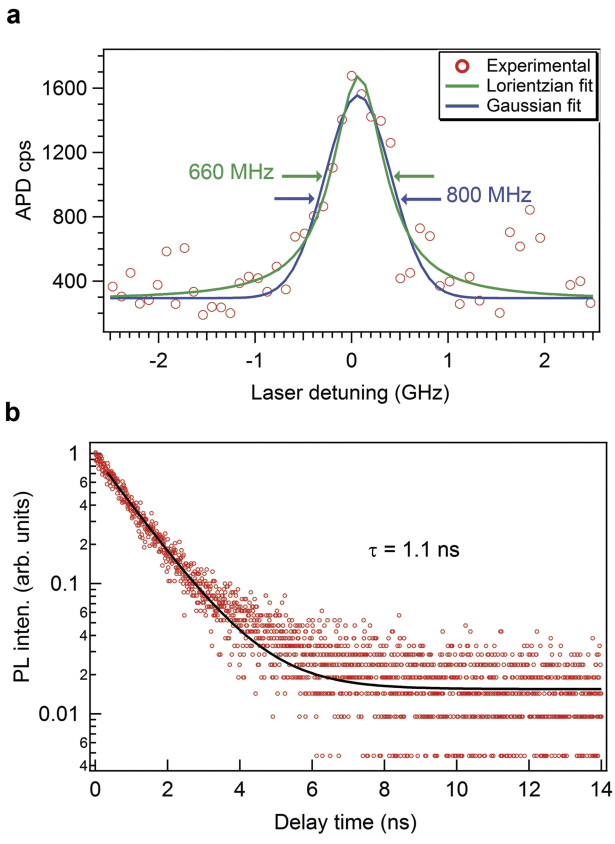

FIG. 3. (a) Resonant photoluminescence excitation measurements on the single emitter with a ZPL peak at 779.61 nm. The excitation power used was 5 μW. Only photons from the PSB were collected using a long-pass filter. The experimental data are plotted as open red circles. The data were fit with either a Lorentzian (green line) or Gaussian (blue line) function. The measurement was done at 10 K. (b) Time-resolved PL measurements (red open circles) of the same single emitter measured at room temperature. A single-exponential fit gives rise to a lifetime of 1.1 ns for the emitter's excited state. The measurement was done with a 675-nm pulsed laser (100 μW, 10-MHz repetition rate, 100-ps pulse width).

The linewidth broadening can arise from numerous factors including ultrafast spectral diffusion due to interaction of the strong emitter dipole with fluctuating electric fields from surrounding defects (inhomogeneous broadening), or alternatively, a homogeneous broadening due to phonon coupling. In addition, spectral diffusion often results in intensity fluctuations, associated with slow frequency jumps, which were not observed in our experiments. Based on these considerations, combined with the more favorable Lorentzian fit, we conclude that the line broadening is predominantly due to phonon interactions. Similar behaviors were also reported for the SiV[15,36] and the GeV[18] in diamonds. Despite the line broadening, achieving a sub-GHz linewidth from single emitters in nanodiamonds—particularly at the NIR spectral range—is valuable, as it opens pathways to coupling these emitters to high-quality optical resonators and photonic cavities.[24,25]

Next, we measured the emitter's linewidth off-resonantly as a function of laser power to determine the photostability of the emitter under increasing excitation power. Figures 4(a) and 4(b) show the optical stability of the emitters under a relatively low 300-μW and high 3-mW excitation laser power, respectively. For these measurements, a total of 200 PL spectra were acquired at intervals of 200 ms. At low power (300 μW), almost no spectral diffusion or blinking to a different frequency was witnessed (within the spectrometer resolution). Conversely, at the higher excitation power of ~3 mW, the spectral fluctuation of the ZPL became noticeable. Spectral jumps as large as ~1.5 nm away from the ZPL position were observed, which are several orders of magnitude higher than the measured FWHM of ~660 MHz. This suggests that the emitter is highly susceptible to the strength of the laser electromagnetic field, and it may possess a linear permanent dipole behavior that may result in spectral diffusion under increased excitation power. Additionally, an increased pumping intensity may result in photoionization—similarly to what occurs with the NV center.[37] Photoionization will result in a frequency drift and can be evidenced as blinking. Note, however, that the spectral jumps occurred on the time scale of seconds, which means techniques such as dynamic stabilization using applied electric fields can be employed to stabilize the emitter under high excitation power.[38]

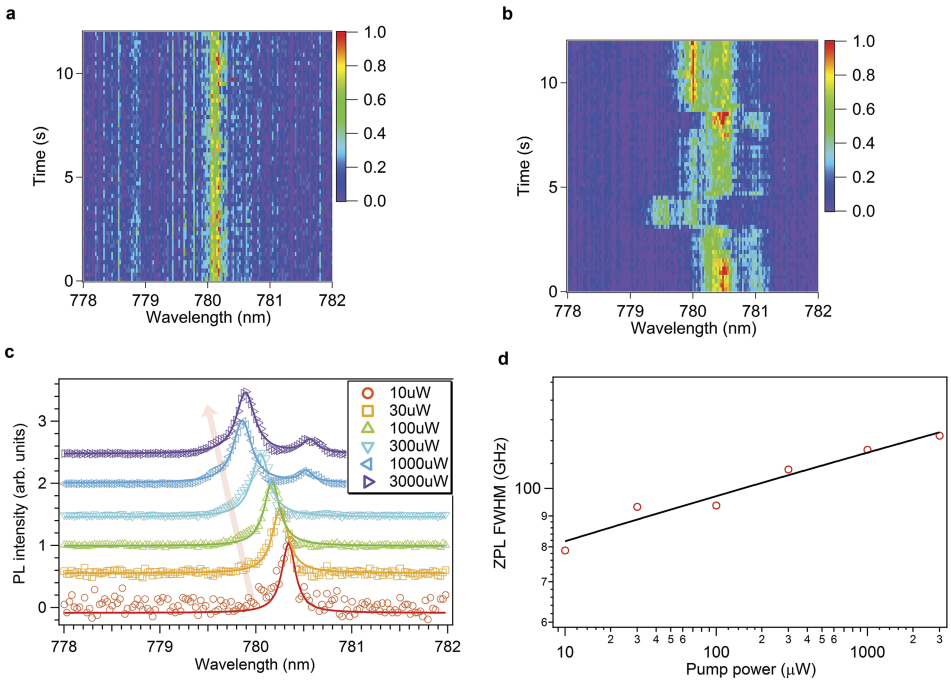

FIG. 4. Spectral stability measurements taken from the emitter at 300 μW (a) and 3 mW (b). All the spectra shown were normalized. (c) Power-induced linewidth broadening measurements for the same emitter with laser power increasing from 10 μW to 3 mW. The open markers and solid lines are experimental and fit data, respectively. The red semitransparent arrow serves as a guide to the eye for the shift in the spectra. (d) Lorentzian-fit FWHM of the linewidth of the emitter with respect to the pump power from (c). The data are fit to a power function. The spectral broadening is evident.

In addition to the power induced blinking, the ZPL exhibits broadening as a function of excitation power. Figure 4(c) shows several spectra from the same SPE under increased excitation powers which reveal power broadening and a blue shift in the ZPL spectral positions. Figure 4(d) presents a plot of the FWHM values as a function of power, showing a good fit with a power function that was employed previously for defects in solids.[39] These measurements are also in agreement with previous optical studies on carbon nanotubes, suggesting that the broadening arises from an increase of the local temperature induced by an increase in power of the excitation laser.[40]

Finally, we discuss the potential origin of the emitters. Amongst color centers in diamonds, only SiV, GeV, and an unknown NIR defect[22] exhibited narrow lines amenable to resonant excitation. While we cannot categorically exclude that the emitters are highly detuned SiV defects, we do not believe that this is the case for the following reasons: (1) we have not observed splitting into 4 spectral lines at cryogenic temperatures—a typical signature of a single SiV defect, even under high strain environment as reported by Evans *et al.*[41] Indeed, some cases report that not all SiV defects exhibit splitting[31,42] but majority of them do. In our case, no splitting was observed in any of the lines. (2) The studied emitter's ZPL at ~780 nm is also far from the standard SiV emission centered at 738 nm.[14] While detuned single SiVs were observed at ~750–760 nm range,[43,44] there is no clear indication that single negatively charged SiVs can have ZPLs farther in the NIR. Previous reports by Neu *et al.*[45] suggested that another NIR transition of the SiV exists, but this is much weaker than the main transition, in stark contrast to our observation as shown in Fig. 1(b). (3) We clearly observe single bright emitters in addition to the ensemble of weak SiVs. While previous reports showed that single SiVs can emit at wavelengths higher than 738 nm,[43,45] there is no evidence for single-photon emission from these lines when an additional ensemble of SiV emitters is present, nor there is a proof that these additional lines are in fact SiV defects.

The observed emitters in our work could be attributed to Cr-related impurities, as the sample was grown on sapphire, in accordance with a similar procedure reported in previous studies,[46] although previous measurements from these emitters revealed broader GHz lines.[22] The incorporation of chromium can occur during the growth since the plasma slightly etches the sapphire allowing the chromium atoms to diffuse into the diamond during growth. Another viable explanation is the recently discovered narrowband emitters that appear at secondary nucleation sites and extended defects in CVD-grown nanodiamonds.[47] As seen from the SEM image in Fig. 1(a), many nanodiamonds possess such defects and therefore give rise to the narrowband PL lines, as indeed observed in our experiments. The attribution of these lines to the morphological defects is therefore plausible and offers advantage since such nanodiamonds can be easily grown in standard laboratory settings. This is, for instance, easier than growing nanodiamonds containing GeVs or SiVs as they require specific doping control. The presented emitters are also slightly brighter than the currently available nanodiamonds hosting SiVs (with exception of NDs grown on iridium) and GeVs. While we cannot conclusively identify the origin of the emitters, the production of these emitters from standard growth offers the unique opportunity to explore quantum optics experiments and relevant applications with single nanodiamond emitters in the NIR.

IV. CONCLUSION

In conclusion, our study shows promising optical properties of SPEs with ZPLs at the NIR (~780 nm). The resonant excitation measurements suggest that the SPE has a FWHM of ~660 MHz, broadened likely by interactions with phonons. The studied emitter does not show any blinking under resonant excitation and low power excitation. The SPE exhibits high DW factors exceeding 0.85, with fast florescence lifetime and fully polarized emission. Our results should stimulate more studies into the promising attributes of NIR emitters in nanodiamonds and their use in quantum photonics applications.

ACKNOWLEDGMENTS

Financial support from the Australian Research Council (No. DE130100592), and the Asian Office of Aerospace Research and Development Grant No. FA2386-17-1-4064 is gratefully

acknowledged. I. A. acknowledges the generous support via the Alexander von Humboldt foundation. This research is supported in part by an Australian Government Research Training Program (RTP) Scholarship.

[1] P. Lodahl, S. Mahmoodian, and S. Stobbe, "Interfacing single photons and single quantum dots with photonic nanostructures," Rev. Mod. Phys. **87**(2), 347–400 (2015).
[2] I. Aharonovich, D. Englund, and M. Toth, "Solid-state single-photon emitters," Nat. Photonics **10**(10), 631–641 (2016).
[3] M. J. Holmes, K. Choi, S. Kako, M. Arita, and Y. Arakawa, "Room-temperature triggered single photon emission from a III-nitride site-controlled nanowire quantum dot," Nano Lett. **14**(2), 982–986 (2014).
[4] H. Wang, Y. He, Y.-H. Li, Z.-E. Su, B. Li, H.-L. Huang, X. Ding, M.-C. Chen, C. Liu, J. Qin, J.-P. Li, Y.-M. He, C. Schneider, M. Kamp, C.-Z. Peng, S. Höfling, C.-Y. Lu, and J.-W. Pan, "High-efficiency multiphoton boson sampling," Nat. Photonics **11**(6), 361–365 (2017).
[5] E. Togan, Y. Chu, A. S. Trifonov, L. Jiang, J. Maze, L. Childress, M. V. G. Dutt, A. S. Sorensen, P. R. Hemmer, A. S. Zibrov, and M. D. Lukin, "Quantum entanglement between an optical photon and a solid-state spin qubit," Nature **466**(7307), 730–734 (2010).
[6] A. Sipahigil, R. E. Evans, D. D. Sukachev, M. J. Burek, J. Borregaard, M. K. Bhaskar, C. T. Nguyen, J. L. Pacheco, H. A. Atikian, C. Meuwly, R. M. Camacho, F. Jelezko, E. Bielejec, H. Park, M. Lončar, and M. D. Lukin, "An integrated diamond nanophotonics platform for quantum optical networks," Science **354**(6314), 847–850 (2016).
[7] H. Bernien, B. Hensen, W. Pfaff, G. Koolstra, M. S. Blok, L. Robledo, T. H. Taminiau, M. Markham, D. J. Twitchen, L. Childress, and R. Hanson, "Heralded entanglement between solid-state qubits separated by three metres," Nature **497**(7447), 86–90 (2013).
[8] F. Jelezko and J. Wrachtrup, "Single defect centres in diamond: A review," Phys. Status Solidi A **203**(13), 3207–3225 (2006).
[9] B. J. M. Hausmann, B. Shields, Q. M. Quan, P. Maletinsky, M. McCutcheon, J. T. Choy, T. M. Babinec, A. Kubanek, A. Yacoby, M. D. Lukin, and M. Loncar, "Integrated diamond networks for quantum nanophotonics," Nano Lett. **12**(3), 1578–1582 (2012).
[10] S. L. Mouradian and D. Englund, "A tunable waveguide-coupled cavity design for scalable interfaces to solid-state quantum emitters," APL Photonics **2**(4), 046103 (2017).
[11] D. Englund, B. Shields, K. Rivoire, F. Hatami, J. Vuckovic, H. Park, and M. D. Lukin, "Deterministic coupling of a single nitrogen vacancy center to a photonic crystal cavity," Nano Lett. **10**(10), 3922–3926 (2010).
[12] B. Pingault, D.-D. Jarausch, C. Hepp, L. Klintberg, J. N. Becker, M. Markham, C. Becher, and M. Atatüre, "Coherent control of the silicon-vacancy spin in diamond," Nat. Commun. **8**, 15579 (2017).
[13] T. Muller, C. Hepp, B. Pingault, E. Neu, S. Gsell, M. Schreck, H. Sternschulte, D. Steinmuller-Nethl, C. Becher, and M. Atatüre, "Optical signatures of silicon-vacancy spins in diamond," Nat. Commun. **5**, 3328 (2014).
[14] E. Neu, D. Steinmetz, J. Riedrich-Möller, S. Gsell, M. Fischer, M. Schreck, and C. Becher, "Single photon emission from silicon-vacancy colour centres in chemical vapour deposition nano-diamonds on iridium," New J. Phys. **13**(2), 025012 (2011).
[15] Y. Zhou, A. Rasmita, K. Li, Q. Xiong, I. Aharonovich, and W.-b. Gao, "Coherent control of a strongly driven silicon vacancy optical transition in diamond," Nat. Commun. **8**, 14451 (2017).
[16] J. N. Becker, J. Gorlitz, C. Arend, M. Markham, and C. Becher, "Ultrafast all-optical coherent control of single silicon vacancy colour centres in diamond," Nat. Commun. **7**, 13512 (2016).
[17] U. Jantzen, A. B. Kurz, D. S. Rudnicki, C. Schäfermeier, K. D. Jahnke, U. L. Andersen, V. A. Davydov, V. N. Agafonov, A. Kubanek, L. J. Rogers, and F. Jelezko, "Nanodiamonds carrying silicon-vacancy quantum emitters with almost lifetime-limited linewidths," New J. Phys. **18**(7), 073036 (2016).
[18] P. Siyushev, M. H. Metsch, A. Ijaz, J. M. Binder, M. K. Bhaskar, D. D. Sukachev, A. Sipahigil, R. E. Evans, C. T. Nguyen, M. D. Lukin, P. R. Hemmer, Y. N. Palyanov, I. N. Kupriyanov, Y. M. Borzdov, L. J. Rogers, and F. Jelezko, "Optical and microwave control of germanium-vacancy center spins in diamond," Phys. Rev. B **96**(8), 081201 (2017).
[19] T. Iwasaki, F. Ishibashi, Y. Miyamoto, Y. Doi, S. Kobayashi, T. Miyazaki, K. Tahara, K. D. Jahnke, L. J. Rogers, B. Naydenov, F. Jelezko, S. Yamasaki, S. Nagamachi, T. Inubushi, N. Mizuochi, and M. Hatano, "Germanium-vacancy single color centers in diamond," Sci. Rep. **5**, 12882 (2015).
[20] V. G. Ralchenko, V. S. Sedov, A. A. Khomich, V. S. Krivobok, S. N. Nikolaev, S. S. Savin, I. I. Vlasov, and V. I. Konov, "Observation of the Ge-vacancy color center in microcrystalline diamond films," Bull. Lebedev Phys. Inst. **42**(6), 165–168 (2015).
[21] D. G. Monticone, P. Traina, E. Moreva, J. Forneris, P. Olivero, I. P. Degiovanni, F. Taccetti, L. Giuntini, G. Brida, G. Amato, and M. Genovese, "Native NIR-emitting single colour centres in CVD diamond," New J. Phys. **16**(5), 053005 (2014).
[22] P. Siyushev, V. Jacques, I. Aharonovich, F. Kaiser, T. Müller, L. Lombez, M. Atatüre, S. Castelletto, S. Prawer, F. Jelezko, and J. Wrachtrup, "Low-temperature optical characterization of a near-infrared single-photon emitter in nanodiamonds," New J. Phys. **11**(11), 113029 (2009).
[23] T. Müller, I. Aharonovich, L. Lombez, Y. Alaverdyan, A. N. Vamivakas, S. Castelletto, F. Jelezko, J. Wrachtrup, S. Prawer, and M. Atatüre, "Wide-range electrical tunability of single-photon emission from chromium-based colour centres in diamond," New J. Phys. **13**(7), 075001 (2011).
[24] A. W. Schell, H. Takashima, S. Kamioka, Y. Oe, M. Fujiwara, O. Benson, and S. Takeuchi, "Highly efficient coupling of nanolight emitters to a ultra-wide tunable nanofibre cavity," Sci. Rep. **5**, 9619 (2015).
[25] O. Benson, "Assembly of hybrid photonic architectures from nanophotonic constituents," Nature **480**(7376), 193–199 (2011).
[26] S. Kalliakos, Y. Brody, A. Schwagmann, A. J. Bennett, M. B. Ward, D. J. P. Ellis, J. Skiba-Szymanska, I. Farrer, J. P. Griffiths, G. A. C. Jones, D. A. Ritchie, and A. J. Shields, "In-plane emission of indistinguishable photons generated by an integrated quantum emitter," Appl. Phys. Lett. **104**(22), 221109 (2014).

[27] R. B. Patel, A. J. Bennett, K. Cooper, P. Atkinson, C. A. Nicoll, D. A. Ritchie, and A. J. Shields, "Postselective two-photon interference from a continuous nonclassical stream of photons emitted by a quantum dot," Phys. Rev. Lett. **100**(20), 207405 (2008).
[28] E. Neu, M. Agio, and C. Becher, "Photophysics of single silicon vacancy centers in diamond: Implications for single photon emission," Opt. Express **20**(18), 19956–19971 (2012).
[29] A. Beveratos, R. Brouri, T. Gacoin, J.-P. Poizat, and P. Grangier, "Nonclassical radiation from diamond nanocrystals," Phys. Rev. A **64**(6), 061802 (2001).
[30] L. J. Rogers, K. D. Jahnke, T. Teraji, L. Marseglia, C. Muller, B. Naydenov, H. Schauffert, C. Kranz, J. Isoya, L. P. McGuinness, and F. Jelezko, "Multiple intrinsically identical single-photon emitters in the solid state," Nat. Commun. **5**, 4739 (2014).
[31] E. Neu, C. Hepp, M. Hauschild, S. Gsell, M. Fischer, H. Sternschulte, D. Steinmüller-Nethl, M. Schreck, and C. Becher, "Low-temperature investigations of single silicon vacancy colour centres in diamond," New J. Phys. **15**(4), 043005 (2013).
[32] D. Englund, A. Majumdar, A. Faraon, M. Toishi, N. Stoltz, P. Petroff, and J. Vučković, "Resonant excitation of a quantum dot strongly coupled to a photonic crystal nanocavity," Phys. Rev. Lett. **104**(7), 073904 (2010).
[33] Y. Shen, T. M. Sweeney, and H. Wang, "Zero-phonon linewidth of single nitrogen vacancy centers in diamond nanocrystals," Phys. Rev. B **77**(3), 033201 (2008).
[34] B. Lounis and M. Orrit, "Single-photon sources," Rep. Prog. Phys. **68**(5), 1129–1179 (2005).
[35] S. Buckley, K. Rivoire, and J. Vučković, "Engineered quantum dot single-photon sources," Rep. Prog. Phys. **75**(12), 126503 (2012).
[36] K. Li, Y. Zhou, A. Rasmita, I. Aharonovich, and W. B. Gao, "Nonblinking emitters with nearly lifetime-limited linewidths in CVD nanodiamonds," Phys. Rev. Appl. **6**(2), 024010 (2016).
[37] N. Aslam, G. Waldherr, P. Neumann, F. Jelezko, and J. Wrachtrup, "Photo-induced ionization dynamics of the nitrogen vacancy defect in diamond investigated by single-shot charge state detection," New J. Phys. **15**(1), 013064 (2013).
[38] V. M. Acosta, C. Santori, A. Faraon, Z. Huang, K. M. C. Fu, A. Stacey, D. A. Simpson, K. Ganesan, S. Tomljenovic-Hanic, A. D. Greentree, S. Prawer, and R. G. Beausoleil, "Dynamic stabilization of the optical resonances of single nitrogen-vacancy centers in diamond," Phys. Rev. Lett. **108**(20), 206401 (2012).
[39] X. Li, G. D. Shepard, A. Cupo, N. Camporeale, K. Shayan, Y. Luo, V. Meunier, and S. Strauf, "Nonmagnetic quantum emitters in boron nitride with ultranarrow and sideband-free emission spectra," ACS Nano **11**(7), 6652–6660 (2017).
[40] C. Galland, A. Högele, H. E. Türeci, and A. Imamoğlu, "Non-markovian decoherence of localized nanotube excitons by acoustic phonons," Phys. Rev. Lett. **101**(6), 067402 (2008).
[41] R. E. Evans, A. Sipahigil, D. D. Sukachev, A. S. Zibrov, and M. D. Lukin, "Narrow-linewidth homogeneous optical emitters in diamond nanostructures via silicon ion implantation," Phys. Rev. Appl. **5**(4), 044010 (2016).
[42] H. Sternschulte, K. Thonke, R. Sauer, P. C. Münzinger, and P. Michler, "1.681-eV luminescence center in chemical-vapor-deposited homoepitaxial diamond films," Phys. Rev. B **50**(19), 14554–14560 (1994).
[43] E. Neu, C. Arend, E. Gross, F. Guldner, C. Hepp, D. Steinmetz, E. Zscherpel, S. Ghodbane, H. Sternschulte, D. Steinmüller-Nethl, Y. Liang, A. Krueger, and C. Becher, "Narrowband fluorescent nanodiamonds produced from chemical vapor deposition films," Appl. Phys. Lett. **98**(24), 243107 (2011).
[44] J. Benedikter, H. Kaupp, T. Hümmer, Y. Liang, A. Bommer, C. Becher, A. Krueger, J. M. Smith, T. W. Hänsch, and D. Hunger, "Cavity-enhanced single-photon source based on the silicon-vacancy center in diamond," Phys. Rev. Appl. **7**(2), 024031 (2017).
[45] E. Neu, R. Albrecht, M. Fischer, S. Gsell, M. Schreck, and C. Becher, "Electronic transitions of single silicon vacancy centers in the near-infrared spectral region," Phys. Rev. B **85**(24), 245207 (2012).
[46] I. Aharonovich, S. Castelletto, D. A. Simpson, A. Stacey, J. McCallum, A. D. Greentree, and S. Prawer, "Two-level ultrabright single photon emission from diamond nanocrystals," Nano Lett. **9**(9), 3191–3195 (2009).
[47] K. Bray, R. Sandstrom, C. Elbadawi, M. Fischer, M. Schreck, O. Shimoni, C. Lobo, M. Toth, and I. Aharonovich, "Localization of narrowband single photon emitters in nanodiamonds," ACS Appl. Mater. Interfaces **8**(11), 7590–7594 (2016).